Supplementary Material for

Cryo-EM structure of DNA-bound Smc5/6 reveals DNA clamping enabled by multi-subunit conformational changes

You Yu[1#], Shibai Li[2#], Zheng Ser[3], Huihui Kuang[4], Thane Than[2], Danying Guan[2], Xiaolan Zhao[2*] and Dinshaw J. Patel[1*]

[1] Structural Biology Program, Memorial Sloan-Kettering Cancer Center, New York, NY, 10065, USA

[2] Molecular Biology Program, Memorial Sloan-Kettering Cancer Center, New York, NY, 10065, USA

[3] Functional Proteomics Laboratory, Institute of Molecular and Cell Biology, Agency for Science, Technology and Research (A*STAR), Singapore 138673, Singapore

[4] Simons Electron Microscopy Center, New York Structural Biology Center, New York, NY, 10027, USA

co-first authors

[*] Corresponding authors: zhaox1@mskcc.org (X.Z.) and pateld@mskcc.org (D.J.P.)

Supplementary Figure Legends

Fig. S1. Sample preparation of 6-subunit *S. cerevisiae* Smc5/6-E/Q complex. Sizing column (Superose 6 increase) elution profile and Coomassie stained gel picture showing the Smc5/6 subunits in the peak fraction and the EM samples containing the complex, dsDNA, and ATP.

Fig. S2. Cryo-EM reconstruction of DNA-bound Smc5/6 complex. (*A*) Workflow of cryo-EM image processing for the complex. (*B*) Global Fourier Shell Correlation (FSC) curve of the complex. The curve for the two half datasets is in blue and that for the refined model versus the cryo-EM map is in red. The overall cryo-EM map resolution is 3.8 Å with FSC set at 0.143. (*C*) Angular distribution plot of final 3D EM map for the complex. (*D*) Final 3D reconstructed map of the complex colored according to local resolution.

Fig. S3. Side chain identification in the cryo-EM structure of DNA-bound Smc5/6 and structural details. (*A*) A view of the complex in ribbon representation with density map shown as a transparent surface. Inserts outline examples where amino acid side chains can be fitted in the density map. (*B, C*) An electron density representation (B) and a ribbon representation (C) of the DNA-bound Smc5/6 structure. These views are rotated 180º compared with those in Figure 1B and 1C. (*D*) "Engaged" Smc1 and Smc3 head domains in the structure of cohesion in the ATP- and DNA-bound Smc1/3-E/Q complex (PDB: 6zz6)[1]. (*E*) "Juxtaposed" Smc2 and Smc4 head domains in the structure of apo-condensin (PDB: 6YVU)[2].

Fig. S4. Sequence alignment and comparison of Nse3 proteins from *X. laevis* and *S. cerevisiae*. (*A*) Sequence alignments between the Nse3 domains of *S. cerevisiae* and *X. laevis.* Residues involved in hydrogen bond interactions with DNA are marked by stars for the Nse3-patch 1 region (blue) and the Nse3-mediated patch 2 region (green). The linker between the WHA and WHB of Nse3 in yeast contains insertions including a helix (adH) and a loop (WHL). (*B*) Structural overlay between the Nse1-3 and the interacting Nse4 peptide from *X. laevis* (grey) and *S. cerevisiae* (color).

Fig. S5. DNA binding details of the DNA-bound Smc5/6 complex. (*A, B*) Overview of DNA contacts involving Nse3 (patches 1 and 2) and Nse4 (patch 5) (A) and those involving Smc5 (patch 3) and Smc6 (patch 4) (B). Observable Lys and Arg side chains are shown in a ribbon representation, while those whose side chain densities could not be traced are shown in a ball representation.

Fig. S6. CLMS data from DNA-free Smc5/6 mapped to the DNA-bound Smc5/6 structure. Inter-subunit CLs detected among Nse1, Nse3 and Nse4. Red lines indicate CL pairs with Cα-Cα distance exceeding that allowed by crosslinkers, while black lines indicate satisfied CL pairs.

Fig. S7. SMC-DNA clamping in the E-K compartment. The protein subunits are shown in a ribbon representation and the bound dsDNA in a yellow stick representation. (*A*) 3.8 Å cryo-EM structure of dsDNA-bound *S. cerevisiae* Smc5/6-EQ complex (this study). (*B*) 3.4 Å cryo-EM

structure of dsDNA-bound *S. cerevisiae* cohesion-EQ complex (PDB: 6ZZ6)[1]. (*C*) 3.1 Å cryo-EM structure of dsDNA-bound *E. coli* MukBEF-EQ complex (PDB: 7NYW)[3].

References

1. Collier, J. et al. Transport of DNA within cohesin involves clamping on top of engaged heads by Scc2 and entrapment within the ring by Scc3. *elife* **9**, e59560 (2020).
2. Lee, B.-G. et al. Cryo-EM structures of holo condensin reveal a subunit flip-flop mechanism. *Nat Struct Mol Biol* **27**, 743-751 (2020).
3. Burmann, F., Funke, L. F. H., Chin, J. W. & Lowe, J. Cryo-EM structure of MukBEF reveals DNA loop entrapment at chromosomal unloading sites. *Mol Cell* **81**, 4891-4906 (2021).

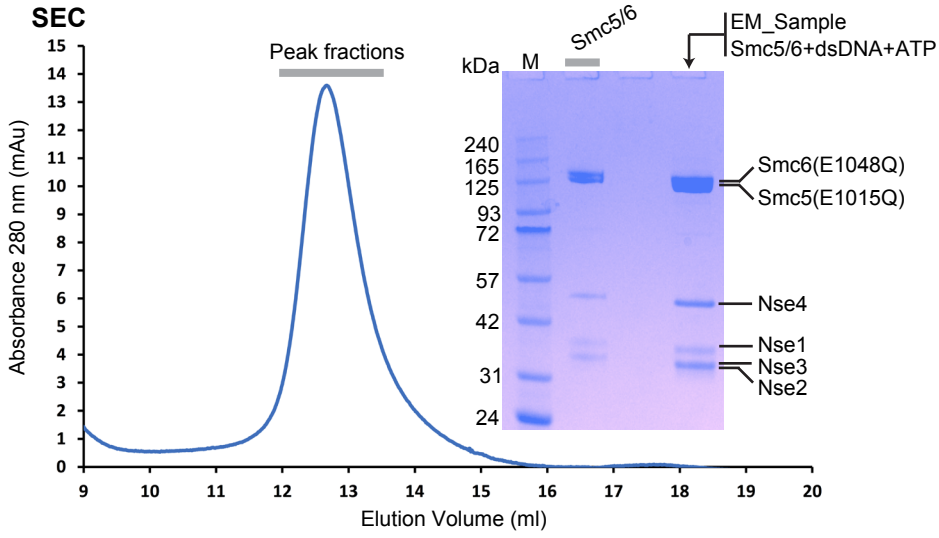
SEC
Peak fractions
Absorbance 280 nm (mAu)
Elution Volume (ml)
kDa
M
Smc5/6
EM_Sample
Smc5/6+dsDNA+ATP
240
165
125
93
72
57
42
31
24
Smc6(E1048Q)
Smc5(E1015Q)
Nse4
Nse1
Nse3
Nse2

Figure S1

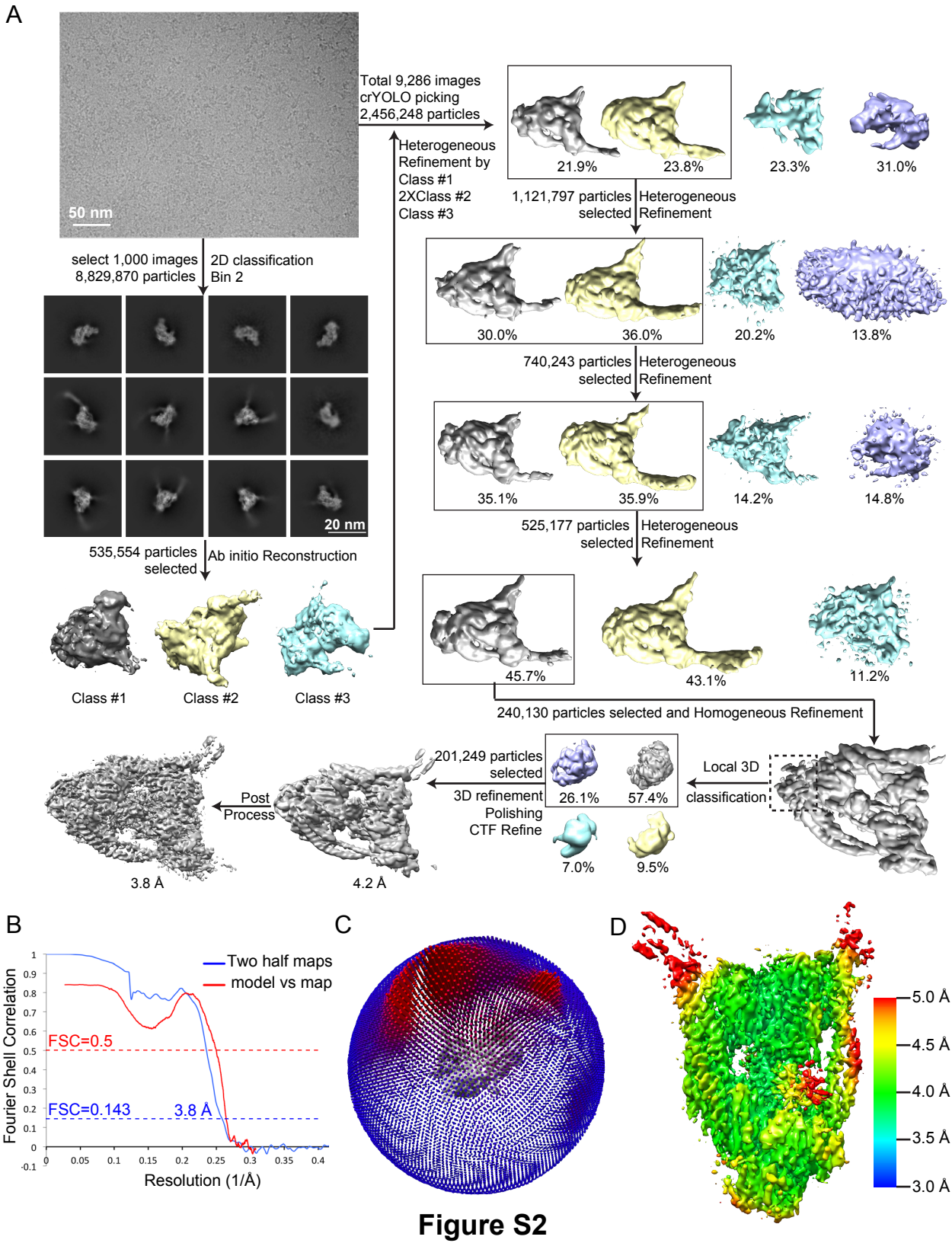
A
50 nm
Total 9,286 images
crYOLO picking
2,456,248 particles
Heterogeneous
Refinement by
Class #1
2XClass #2
Class #3
21.9%
23.8%
23.3%
31.0%
1,121,797 particles
selected
Heterogeneous
Refinement
select 1,000 images
8,829,870 particles
2D classification
Bin 2
30.0%
36.0%
20.2%
13.8%
740,243 particles
selected
Heterogeneous
Refinement
20 nm
35.1%
35.9%
14.2%
14.8%
525,177 particles
selected
Heterogeneous
Refinement
535,554 particles
selected
Ab initio Reconstruction
45.7%
43.1%
11.2%
Class #1
Class #2
Class #3
240,130 particles selected and Homogeneous Refinement
Local 3D
classification
201,249 particles
selected
3D refinement
Polishing
CTF Refine
26.1%
57.4%
7.0%
9.5%
Post
Process
3.8 Å
4.2 Å
B
Two half maps
model vs map
FSC=0.5
FSC=0.143
3.8 Å
Fourier Shell Correlation
Resolution (1/Å)
C
D
5.0 Å
4.5 Å
4.0 Å
3.5 Å
3.0 Å

Figure S2

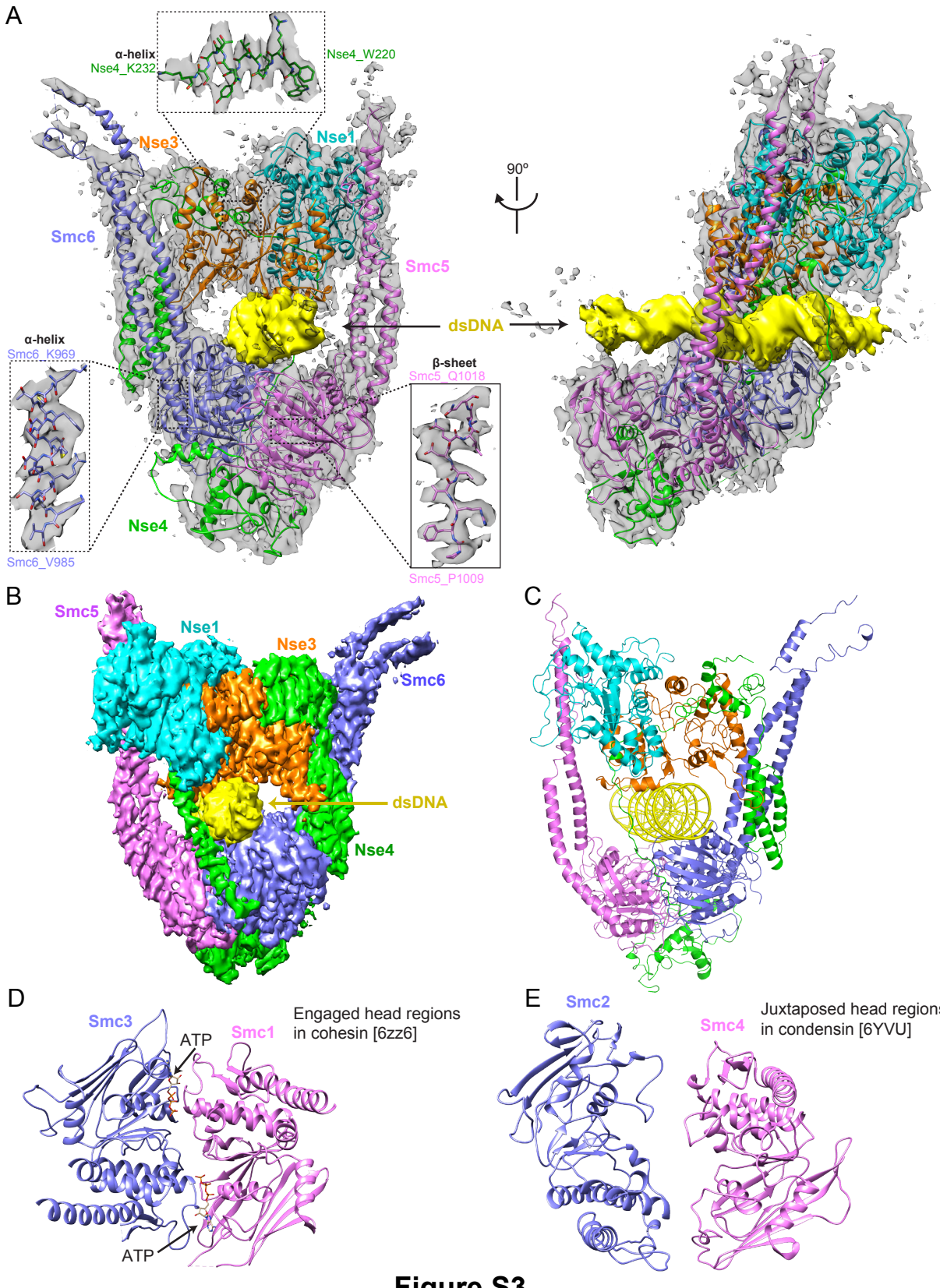
A
α-helix
Nse4_K232
Nse4_W220
Nse3
Nse1
Smc6
Smc5
90°
dsDNA
α-helix
Smc6_K969
β-sheet
Smc5_Q1018
Nse4
Smc6_V985
Smc5_P1009
B
Smc5
Nse1
Nse3
Smc6
dsDNA
Nse4
C
D
Smc3
ATP
Smc1
Engaged head regions
in cohesin [6zz6]
ATP
E
Smc2
Smc4
Juxtaposed head regions
in condensin [6YVU]

Figure S3

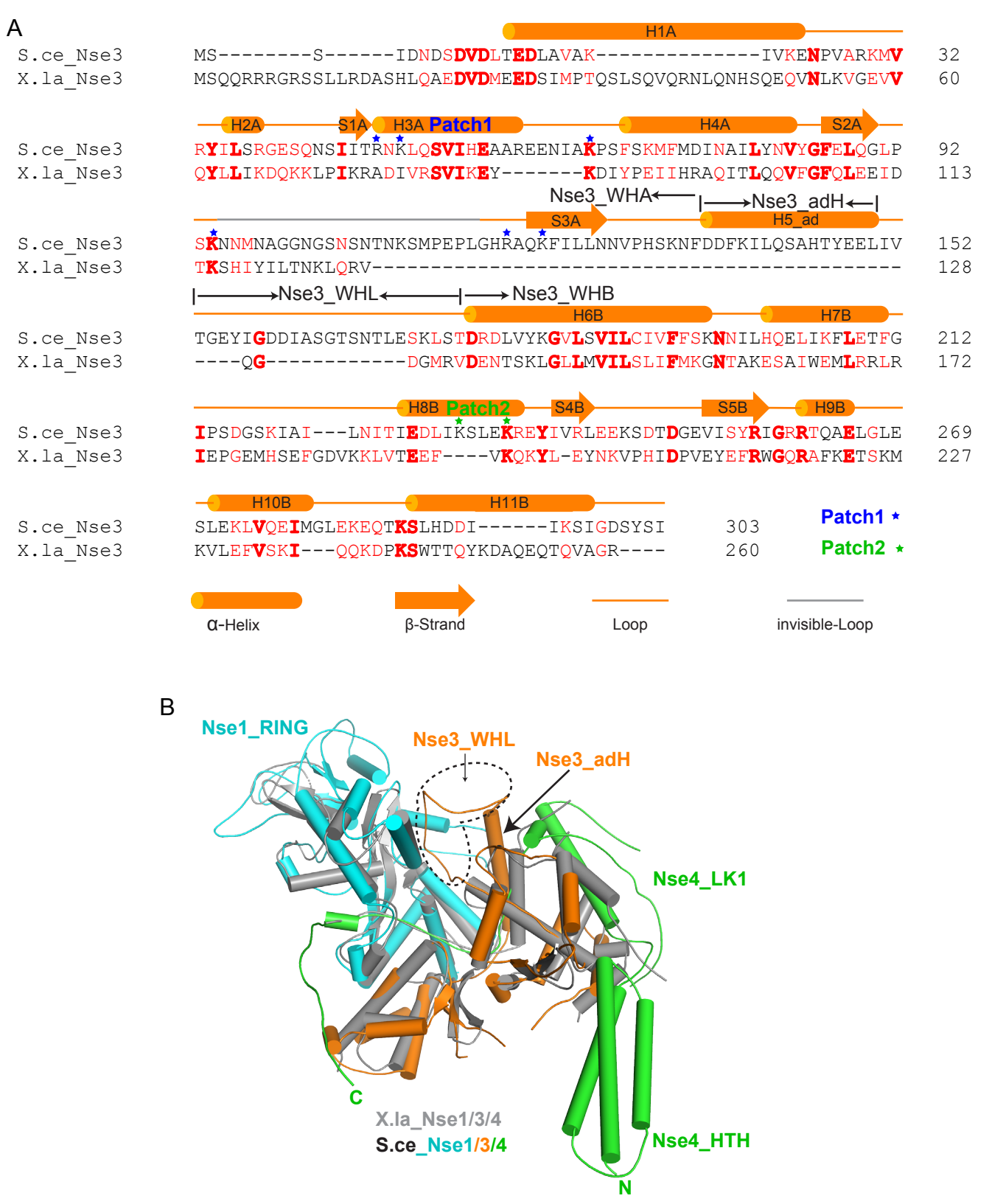
A
H1A
S.ce_Nse3 MS--------S------IDNDSDVDLTEDLAVAK--------------IVKENPVARKMV 32
X.la_Nse3 MSQQRRRGRSSLLRDASHLQAEDVDMEEDSIMPTQSLSQVQRNLQNHSQEQVNLKVGEVV 60
H2A
S1A
H3A Patch1
H4A
S2A
S.ce_Nse3 RYILSRGESQNSIITRNKLQSVIHEAAREENIAKPSFSKMFMDINAILYNVYGFELQGLP 92
X.la_Nse3 QYLLIKDQKKLPIKRADIVRSVIKEY-------KDIYPEIIHRAQITLQQVFGFQLEEID 113
Nse3_WHA
Nse3_adH
S3A
H5_ad
S.ce_Nse3 SKNNMNAGGNGSNSNTNKSMPEPLGHRAQKFILLNNVPHSKNFDDFKILQSAHTYEELIV 152
X.la_Nse3 TKSHIYILTNKLQRV---------- 128
Nse3_WHL
Nse3_WHB
H6B
H7B
S.ce_Nse3 TGEYIGDDIASGTSNTLESKLSTDRDLVYKGVLSVILCIVFFSKNNILHQELIKFLETFG 212
X.la_Nse3 ----QG----------DGMRVDENTSKLGLLMVILSLIFMKGNTAKESAIWEMLRRLR 172
H8B Patch2
S4B
S5B
H9B
S.ce_Nse3 IPSDGSKIAI---LNITIEDLIKSLEKREYIVRLEEKSDTDGEVISYRIGRRTQAELGLE 269
X.la_Nse3 IEPGEMHSEFGDVKKLVTEEF----VKQKYL-EYNKVPHIDPVEYEFRWGQRAFKETSKM 227
H10B
H11B
S.ce_Nse3 SLEKLVQEIMGLEKEQTKSLHDDI------IKSIGDSYSI 303
X.la_Nse3 KVLEFVSKI---QQKDPKSWTTQYKDAQEQTQVAGR---- 260
Patch1
Patch2
α-Helix
β-Strand
Loop
invisible-Loop
B
Nse1_RING
Nse3_WHL
Nse3_adH
Nse4_LK1
C
X.la_Nse1/3/4
S.ce_Nse1/3/4
Nse4_HTH
N

Figure S4

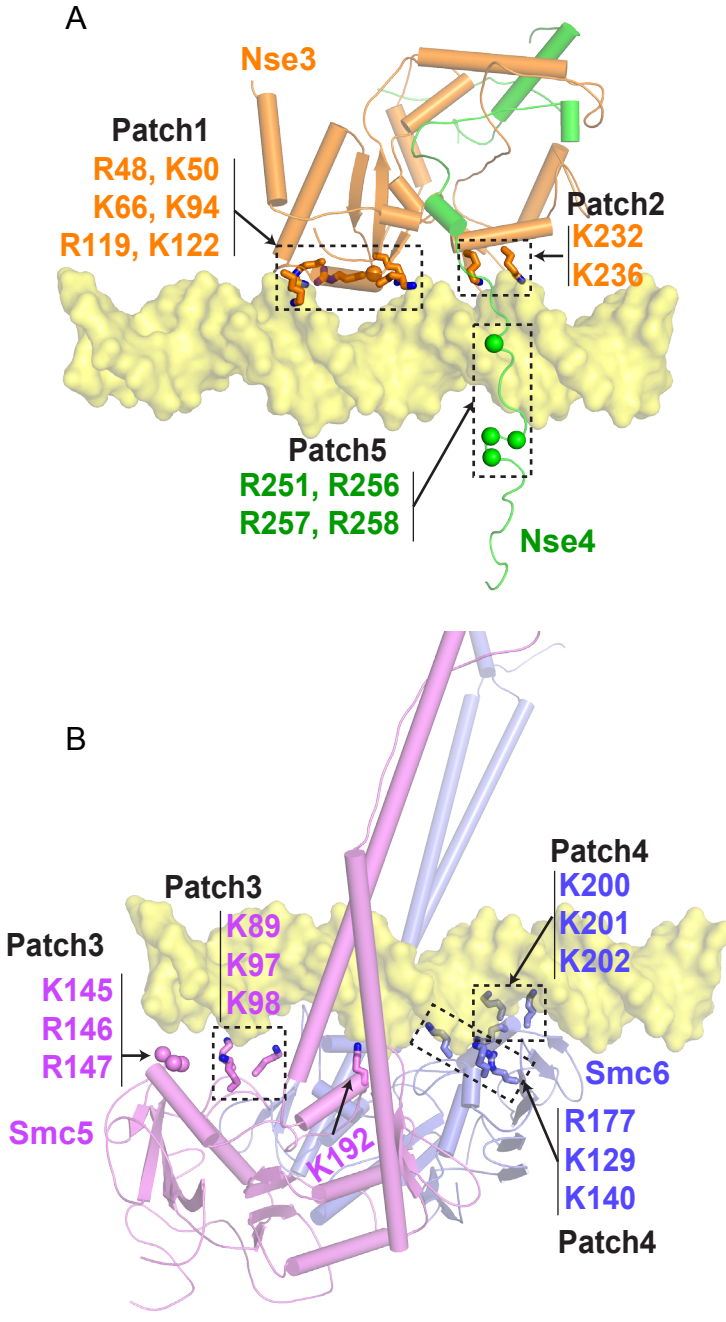
A
Nse3
Patch1
R48, K50
K66, K94
R119, K122
Patch2
K232
K236
Patch5
R251, R256
R257, R258
Nse4
B
Patch4
K200
K201
K202
Patch3
K89
K97
K98
Patch3
K145
R146
R147
Smc6
R177
K129
K140
Patch4
Smc5
K192

Figure S5

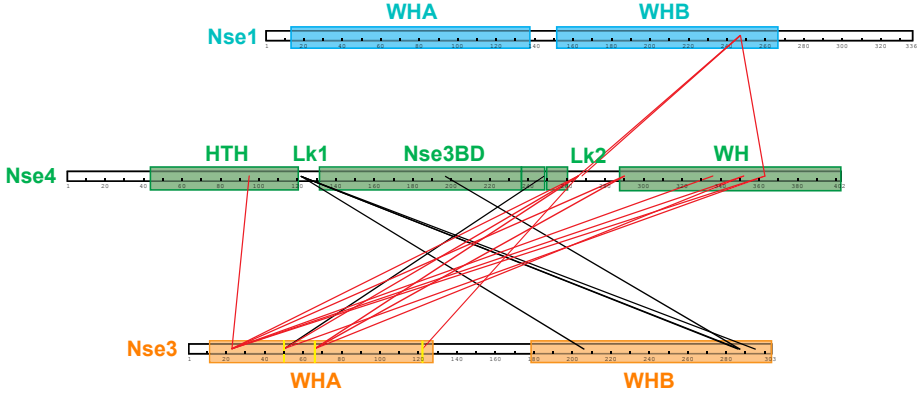

Figure S6

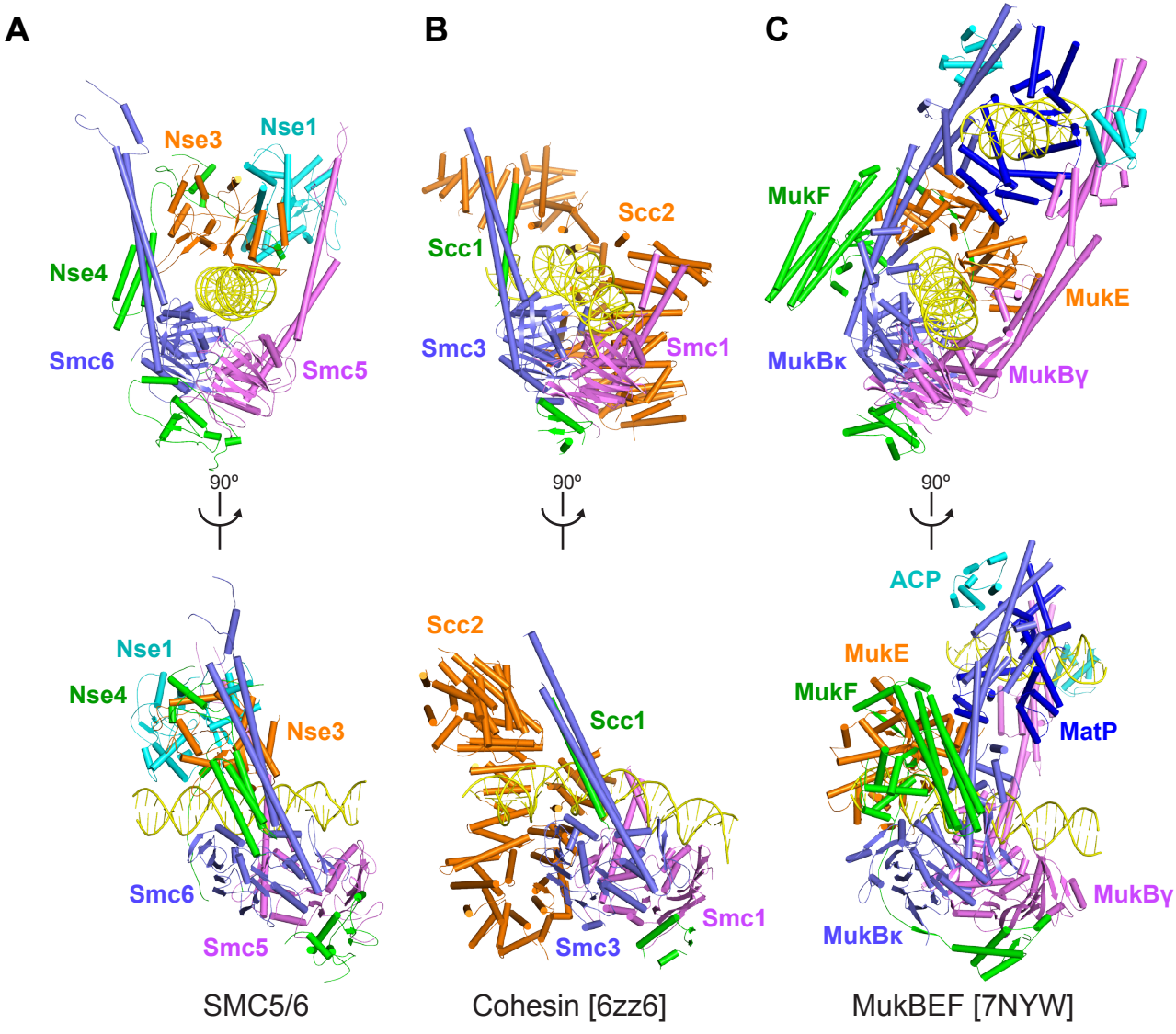
A
Nse3
Nse1
Nse4
Smc6
Smc5
90°
Nse1
Nse4
Nse3
Smc6
Smc5
SMC5/6
B
Scc2
Scc1
Smc3
Smc1
90°
Scc2
Scc1
Smc1
Smc3
Cohesin [6zz6]
C
MukF
MukE
MukBκ
MukBγ
90°
ACP
MukE
MukF
MatP
MukBγ
MukBκ
MukBEF [7NYW]

Figure S7

Table S1. Cryo-EM data collection, processing, and validation statistics

Sample	ATP-dsDNA-SMC5/6 EMD-26140 PDB: 7TVE
Data collection	
Microscope	Titan Krios
Detector	Gatan K3
Automation software	Leginon
Nominal magnification	81,000
Voltage (kV)	300 kV
Total dose ($e^-/Å^2$)	53.55
Dose rate (e^-/pixel/s)	30
Number of frames collected	40
Defocus range (μm)	-0.8 to -2.5
Pixel size (Å)	1.069
Collected Micrographs	9,286
Selected Micrographs	9,286
Reconstruction	
Initially autopicked particles	2,456,248
Particles used for classification	2,456,248
Particles in the final map	201,249
Symmetry	C1
Resolution	
FSC 0.5 (unmasked/masked, Å)	4.1/4.1
FSC 0.143 (unmasked/masked, Å)	3.8/3.8
Map sharpening B factor ($Å^2$)	-138.59
Model composition	
Protein residues	1793
Nonhydrogen atoms	15466
Validation	
MolProbity	2.78
Clash score	17.8
Map Correlation Coefficient	0.69
R.m.s. deviations	
Bond lengths (Å)	0.005
Bond angles (°)	0.827
Ramachandran plots	
Favored (%)	86.28
Allowed (%)	13.44
Outliers (%)	0.28
Rotamer outliers (%)	3.26

Table S2 CLMS analyses results used in this study

Protein 1	Residue 1	Protein 2	Residue 2	CA distance	Threshold	Sat-Viol	inter vs intra	figure panel	dataset
SMC5	248	SMC6	916	78.7	30	V	inter	Figure 6A	Yu et al 2021
SMC5	260	SMC6	906	85.6	30	V	inter	Figure 6A	Yu et al 2021
SMC5	248	SMC6	913	81.5	30	V	inter	Figure 6A	Yu et al 2021
SMC5	260	SMC6	913	78.6	30	V	inter	Figure 6A	Yu et al 2021
SMC5	259	SMC6	913	78.8	30	V	inter	Figure 6A	Yu et al 2021
SMC5	259	SMC6	906	86	30	V	inter	Figure 6A	Yu et al 2021
SMC5	259	SMC6	917	75.9	30	V	inter	Figure 6A	Yu et al 2021
SMC5	248	SMC6	917	77.5	30	V	inter	Figure 6A	Yu et al 2021
SMC5	252	SMC6	913	79	30	V	inter	Figure 6A	Yu et al 2021
SMC5	259	SMC6	913	78.8	25	V	inter	Figure 6A	Taschner et al 2021
SMC5	248	SMC6	913	81.5	25	V	inter	Figure 6A	Taschner et al 2021
SMC5	248	SMC6	921	82.9	25	V	inter	Figure 6A	Taschner et al 2021
SMC5	252	SMC6	913	79	25	V	inter	Figure 6A	Taschner et al 2021
SMC5	249	SMC6	913	79	25	V	inter	Figure 6A	Taschner et al 2021
NSE3	246	SMC5	909	73	30	V	inter	Figure 6B	Yu et al 2021
NSE3	236	SMC5	919	57.2	25	V	inter	Figure 6B	Taschner et al 2021
NSE3	236	SMC5	980	46.7	25	V	inter	Figure 6B	Taschner et al 2021
NSE3	236	SMC5	979	47.4	25	V	inter	Figure 6B	Taschner et al 2021
NSE3	246	SMC5	919	70.6	25	V	inter	Figure 6B	Taschner et al 2021
NSE3	23	SMC5	980	48.9	25	V	inter	Figure 6B	Taschner et al 2021
NSE3	66	SMC5	980	35.8	25	V	inter	Figure 6B	Taschner et al 2021
NSE3	23	SMC6	281	65.7	25	V	inter	Figure 6B	Taschner et al 2021
NSE4	197	SMC5	235	72.4	25	V	inter	Figure 6B	Taschner et al 2021
NSE4	197	SMC6	281	13.8	25	S	inter	Figure 6B	Taschner et al 2021
NSE1	247	NSE4	266	71	30	V	inter	Figure 6C	Yu et al 2021
NSE1	247	NSE4	268	75.3	30	V	inter	Figure 6C	Yu et al 2021
NSE1	247	NSE4	363	113.8	30	V	inter	Figure 6C	Yu et al 2021
NSE3	23	NSE4	363	85.3	30	V	inter	Figure 6C	Yu et al 2021
NSE3	206	NSE4	122	19.2	30	S	inter	Figure 6C	Yu et al 2021
NSE3	295	NSE4	122	10.3	30	S	inter	Figure 6C	Yu et al 2021
NSE3	23	NSE4	95	70	25	V	inter	Figure 6C	Taschner et al 2021
NSE3	23	NSE4	266	68.4	25	V	inter	Figure 6C	Taschner et al 2021
NSE3	23	NSE4	336	84.5	25	V	inter	Figure 6C	Taschner et al 2021
NSE3	23	NSE4	352	89	25	V	inter	Figure 6C	Taschner et al 2021
NSE3	50	NSE4	266	47	25	V	inter	Figure 6C	Taschner et al 2021
NSE3	50	NSE4	363	72.3	25	V	inter	Figure 6C	Taschner et al 2021
NSE3	**66**	NSE4	266	56.1	25	V	inter	Figure 6C	Taschner et al 2021
NSE3	**66**	NSE4	290	71.1	25	V	inter	Figure 6C	Taschner et al 2021
NSE3	**66**	NSE4	352	75.6	25	V	inter	Figure 6C	Taschner et al 2021
NSE3	**122**	NSE4	266	51.7	25	V	inter	Figure 6C	Taschner et al 2021
NSE3	50	NSE4	248	24.1	25	S	inter	Figure 6C	Taschner et al 2021
NSE3	286	NSE4	122	22.7	25	S	inter	Figure 6C	Taschner et al 2021
NSE3	287	NSE4	122	23	25	S	inter	Figure 6C	Taschner et al 2021
NSE3	287	NSE4	197	15.2	25	S	inter	Figure 6C	Taschner et al 2021
NSE4	95	NSE4	122	43.3	25	V	intra	Figure 6D	Taschner et al 2021
NSE4	248	NSE4	266	47.2	25	V	intra	Figure 6D	Taschner et al 2021
NSE4	266	NSE4	285	40.6	25	V	intra	Figure 6D	Taschner et al 2021
NSE4	266	NSE4	290	49.1	25	V	intra	Figure 6D	Taschner et al 2021
NSE4	266	NSE4	352	62.6	25	V	intra	Figure 6D	Taschner et al 2021
NSE4	266	NSE4	363	65.2	25	V	intra	Figure 6D	Taschner et al 2021
NSE4	268	NSE4	333	48.9	25	V	intra	Figure 6D	Taschner et al 2021
NSE4	268	NSE4	363	60.3	25	V	intra	Figure 6D	Taschner et al 2021
SMC5	235	SMC5	915	28.3	30	S	intra	Figure 6E	Yu et al 2021
SMC5	235	SMC5	909	22.9	30	S	intra	Figure 6E	Yu et al 2021
SMC5	248	SMC5	260	18.5	30	S	intra	Figure 6E	Yu et al 2021
SMC5	248	SMC5	259	16.7	30	S	intra	Figure 6E	Yu et al 2021
SMC5	227	SMC5	235	12.7	30	S	intra	Figure 6E	Yu et al 2021
SMC5	252	SMC5	260	12.5	30	S	intra	Figure 6E	Yu et al 2021

SMC5	111	SMC5	136	12.4	30	S	intra	Figure 6E	Yu et al 2021
SMC5	192	SMC5	980	11.7	30	S	intra	Figure 6E	Yu et al 2021
SMC5	252	SMC5	259	10.6	30	S	intra	Figure 6E	Yu et al 2021
SMC5	44	SMC5	136	10.2	30	S	intra	Figure 6E	Yu et al 2021
SMC5	971	SMC5	980	9.1	30	S	intra	Figure 6E	Yu et al 2021
SMC5	971	SMC5	979	6.7	30	S	intra	Figure 6E	Yu et al 2021
SMC5	245	SMC5	249	6.2	30	S	intra	Figure 6E	Yu et al 2021
SMC5	915	SMC5	919	6.1	30	S	intra	Figure 6E	Yu et al 2021
SMC5	245	SMC5	248	4.9	30	S	intra	Figure 6E	Yu et al 2021
SMC5	232	SMC5	235	4.7	30	S	intra	Figure 6E	Yu et al 2021
SMC6	288	SMC6	304	24.9	30	S	intra	Figure 6E	Yu et al 2021
SMC6	987	SMC6	1070	22.6	30	S	intra	Figure 6E	Yu et al 2021
SMC6	943	SMC6	958	22.6	30	S	intra	Figure 6E	Yu et al 2021
SMC6	989	SMC6	1059	18.8	30	S	intra	Figure 6E	Yu et al 2021
SMC6	987	SMC6	1067	18.1	30	S	intra	Figure 6E	Yu et al 2021
SMC6	1067	SMC6	1087	17.3	30	S	intra	Figure 6E	Yu et al 2021
SMC6	1059	SMC6	1070	17.1	30	S	intra	Figure 6E	Yu et al 2021
SMC6	987	SMC6	1059	15.3	30	S	intra	Figure 6E	Yu et al 2021
SMC6	1059	SMC6	1087	13.7	30	S	intra	Figure 6E	Yu et al 2021
SMC6	83	SMC6	160	13.4	30	S	intra	Figure 6E	Yu et al 2021
SMC6	1059	SMC6	1081	12.4	30	S	intra	Figure 6E	Yu et al 2021
SMC6	965	SMC6	996	12	30	S	intra	Figure 6E	Yu et al 2021
SMC6	1070	SMC6	1077	11.5	30	S	intra	Figure 6E	Yu et al 2021
SMC6	901	SMC6	906	11.2	30	S	intra	Figure 6E	Yu et al 2021
SMC6	958	SMC6	965	10.8	30	S	intra	Figure 6E	Yu et al 2021
SMC6	906	SMC6	913	10.7	30	S	intra	Figure 6E	Yu et al 2021
SMC6	1067	SMC6	1070	5.3	30	S	intra	Figure 6E	Yu et al 2021
NSE1	97	NSE1	247	18.2	30	S	intra	Figure 6F	Yu et al 2021
NSE1	99	NSE1	243	19.1	30	S	intra	Figure 6F	Yu et al 2021
NSE3	23	NSE3	66	14.2	25	S	intra	Figure 6F	Taschner et al 2021
NSE3	50	NSE3	66	15.8	25	S	intra	Figure 6F	Taschner et al 2021
NSE3	50	NSE3	122	9.5	25	S	intra	Figure 6F	Taschner et al 2021
NSE3	50	NSE3	236	17.1	25	S	intra	Figure 6F	Taschner et al 2021
NSE3	53	NSE3	66	12.6	25	S	intra	Figure 6F	Taschner et al 2021
NSE3	66	NSE3	122	20.7	25	S	intra	Figure 6F	Taschner et al 2021
NSE3	122	NSE3	236	14.2	25	S	intra	Figure 6F	Taschner et al 2021
NSE3	133	NSE3	283	13.6	25	S	intra	Figure 6F	Taschner et al 2021